Bridging the *μ*Hz Gap in the Gravitational-Wave Landscape with Binary Resonances

Diego Blas[1,2,3] and Alexander C. Jenkins[3,*]

[1]*Grup de Física Teòrica, Departament de Física, Universitat Autònoma de Barcelona, 08193 Bellaterra, Spain*
[2]*Institut de Fisica d'Altes Energies (IFAE), The Barcelona Institute of Science and Technology, Campus UAB, 08193 Bellaterra, Spain*
[3]*Theoretical Particle Physics and Cosmology Group, Physics Department, King's College London,
University of London, Strand, London WC2R 2LS, United Kingdom*

Gravitational-wave (GW) astronomy is transforming our understanding of the Universe by probing phenomena invisible to electromagnetic observatories. A comprehensive exploration of the GW frequency spectrum is essential to fully harness this potential. Remarkably, current methods have left the *μ*Hz frequency band almost untouched. Here, we show that this *μ*Hz gap can be filled by searching for deviations in the orbits of binary systems caused by their resonant interaction with GWs. In particular, we show that laser ranging of the Moon and artificial satellites around the Earth, as well as timing of binary pulsars, may discover the first GW signals in this band, or otherwise set stringent new constraints. To illustrate the discovery potential of these binary resonance searches, we consider the GW signal from a cosmological first-order phase transition, showing that our methods will probe models of the early Universe that are inaccessible to any other near-future GW mission. We also discuss how our methods can shed light on the possible GW signal detected by NANOGrav, either constraining its spectral properties or even giving an independent confirmation.

Introduction.—The direct detection of gravitational waves (GWs) [1] has initiated an exciting new era in astronomy, opening a window onto uncharted phenomena in the Universe. The range of GW frequencies covered by current and future experiments will probe an impressive list of physical processes, from fundamental aspects of the early Universe to late-time astrophysical systems. However, the practical limitations of these experiments leave certain windows in the GW spectrum unexplored. Crucially, these windows may contain signals from new phenomena difficult to observe at other frequencies. It is thus vitally important to cover the GW spectrum as thoroughly as possible.

A well-known gap in the GW landscape occurs at roughly $10^{-7} - 10^{-4}$ Hz, between the sensitive bands of pulsar timing arrays (PTAs) [2–4] and future space-based interferometers such as the Laser Interferometer Space Antenna (LISA) [5]. Accessing these frequencies is challenging, as this requires "detectors" of astronomical scale, which are nonetheless sensitive to the subtle effects of GWs. One proposal is to construct a solar system–sized interferometer [6]; however, such ideas remain futuristic.

Another possibility is to exploit the interaction of GWs with binary systems, an idea that has a long history [7–11] but has yet to be fully explored. Much like in any other system of masses, the passage of GWs through a binary perturbs the separation of the two bodies, leaving imprints on the system's orbit. This effect is particularly pronounced if (i) the duration of the signal is much longer than the binary period and (ii) the GW frequency is an integer multiple of the orbital frequency; the binary then responds resonantly to the GWs, allowing the perturbations to the orbit to accumulate over time. By tracking changes in the binary's orbital parameters with sufficient precision, one can thus search for GWs at a discrete "comb" of frequencies set by the orbital period. For periods ranging from days to years, this allows us to probe the *μ*Hz gap between LISA and PTAs.

We have recently developed a powerful formalism for calculating the evolution of a binary due to resonance with the stochastic GW background (SGWB) [12]: the persistent, broadband signal sourced by the incoherent superposition of GWs from many sources that are too faint or too numerous to be resolved individually. This formalism improves upon previous work [7–11] by capturing the evolution of the entire probability distribution for all six of the binary's orbital parameters. In this Letter, we apply our formalism to explore the SGWB constraints that are possible with high-precision observations of various binary systems. We show that lunar laser ranging (LLR) and timing of binary pulsars can place stringent new bounds on the SGWB intensity in the *μ*Hz band, while satellite laser ranging (SLR) can be used to explore the LISA band in the decade before LISA flies. Our forecast bounds span the entirety of the gap between LISA and PTAs, and are orders of magnitude stronger than all existing direct bounds in this frequency range.

We use units where $c = k_B = 1$, and set the Hubble constant to $H_0 = 67.66$ kms^{-1} Mpc^{-1} [13].

Theoretical background.—In the absence of perturbations, a Newtonian binary system traverses a fixed elliptical orbit, as determined by Kepler's laws. This ellipse is described in terms of six orbital elements: P, the orbital period; e, the eccentricity; I, the inclination; Ω, the longitude of ascending node; ω, the argument of pericenter; and ε, the mean anomaly at epoch. If perturbed, for example by the passage of a GW, the binary will deviate from its Keplerian ellipse, causing its orbital elements to vary. We thus treat these six parameters as functions of time, called the "osculating" orbital elements [12,14].

The SGWB is the most natural target of binary resonance searches, being persistent (rather than transient) and broadband (rather than narrowband). The SGWB is also a highly interesting target, as it encodes the GW emission from a broad range of sources throughout cosmic history. These sources are likely to include unresolved astrophysical systems at low redshift, such as inspiraling compact binaries [15], and may also include a host of more exotic early-Universe sources, including cosmological first-order phase transitions (FOPTs) [16,17], cosmic strings, and inflationary tensor modes [18].

The unpredictable arrival times and phases of GWs from many independent sources make the SGWB inherently random [18], and we therefore cannot hope to predict the exact evolution of the osculating elements for any given binary. We can, however, calculate the statistical properties of this evolution, allowing us to predict the time evolution of the distribution function of the orbital elements, $W(X, t)$, where $X = \{P, e, I, \Omega, \omega, \varepsilon\}$. This is defined such that an integral over any region $\mathcal{X}$ of parameter space gives the corresponding probability for the osculating elements taking those values at time t,

$$\Pr(X \in \mathcal{X} | t) = \int_{\mathcal{X}} dX W(X, t). \tag{1}$$

Assuming the SGWB perturbations are Gaussian, the time evolution of the distribution function follows a nonlinear [19] Fokker-Planck equation [12,20],

$$\frac{\partial W}{\partial t} = -\frac{\partial}{\partial X_i}(D_i^{(1)} W) + \frac{\partial}{\partial X_i}\frac{\partial}{\partial X_j}(D_{ij}^{(2)} W), \tag{2}$$

(with summation over repeated indices implied). Here $D_i^{(1)}$ and $D_{ij}^{(2)}$ are the drift vector and diffusion matrix, functions of the orbital elements encoding the statistical properties of the stochastic perturbations. In our case, these quantities are fully specified by the SGWB intensity spectrum,

$$\Omega_{\text{gw}}(f) \equiv \frac{1}{\rho_c}\frac{d\rho_{\text{gw}}}{d(\ln f)}, \tag{3}$$

which is the energy density in GWs per logarithmic frequency bin, normalized relative to the critical energy density of the Universe, $\rho_c \equiv 3H_0^2/(8\pi G)$. In a companion paper [12], we derive $D_i^{(1)}$ and $D_{ij}^{(2)}$ for a binary immersed in a Gaussian SGWB; both can be written as linear combinations of the SGWB intensity at the binary's harmonic frequencies,

$$D_i^{(1)}(X) = V_i(X) + \sum_{n=1}^{\infty} \mathcal{A}_{n,i}(X)\Omega_{\text{gw}}(n/P),$$

$$D_{ij}^{(2)}(X) = \sum_{n=1}^{\infty} \mathcal{B}_{n,ij}(X)\Omega_{\text{gw}}(n/P). \tag{4}$$

Note that the drift vector also includes a deterministic term V_i accounting for the binary's evolution in the absence of the SGWB. This includes relativistic effects such as the precession of the pericenter ω and the decay of the period P and eccentricity e due to radiation of GWs, which is particularly important to capture in the case of binary pulsars.

To get a sense of how strong we can expect our forecast constraints to be, it is instructive to carry out a back-of-the-envelope calculation in which the rms perturbation to the orbital period after time T is $\sigma_P = \sqrt{2TD_{PP}^{(2)}}$. Taking the LLR case as an example, for a SGWB intensity $\Omega_{\text{gw}} = 10^{-5}$ and an observation period of $T = 15$ yr, this gives $\sigma_P \sim 1$ μs. This corresponds to a rms perturbation to the semimajor axis of $\sigma_a = (2a/3P)\sigma_P \sim 0.1$ mm. Given that each LLR "normal point" measurement determines the Earth-Moon distance to within ~ 3 mm, we see that a campaign of ~ 1000 such measurements should be capable of detecting this signal.

Results and discussion.—Our main results are based on three different high-precision probes of binary orbital dynamics: (i) MSP: Timing of binary millisecond pulsars (MSPs), with periods between $P \approx 1.5$ hr and $P \approx 5.3$ yr [21]; (2) LLR: Laser-ranging measurements of the Moon's orbit around the Earth ($P \approx 27$ days) [22]; and (iii) SLR: Laser-ranging measurements of the orbits of artificial satellites around the Earth, in particular the LAGEOS-1 satellite ($P \approx 3.8$ hr) [23], as this has been regularly producing laser-ranging data for longer than any other satellite mission.

We numerically evolve the first and second moments of the Fokker-Planck equation [Eq. (2)] from delta-function initial conditions for each of these systems using our PYTHON code GWRESONANCE, which we make publicly available in Ref. [24]. This gives a probabilistic model for the orbital elements over time, which we combine with a Fisher-forecasting approach to calculate the expected sensitivity of each binary to the SGWB (see the Supplemental Material [25]).

— $N_{\rm eff}$	— MSPs (2021)	— SLR (2021)	- - LISA	···· NANOGrav CP	
- - $N_{\rm eff}$ (future)	- - MSPs (2038)	- - SLR (2038)	- - AION	···· SMBBHs	
— PPTA	— LLR (2021)	— Cassini	— LVK	···· SMBH mimickers	
- - SKA	- - LLR (2038)	— Earth modes	- - ET	···· Ultralight bosons	
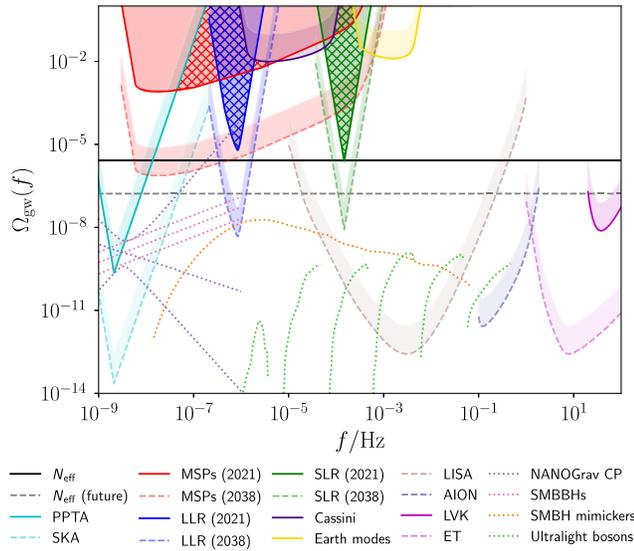
FIG. 1. SGWB sensitivity curves of current and future GW experiments, as well as our forecasts. Each curve is a 95% confidence upper limit (SNR $= 2$), with shaded regions extending up to SNR $= 20$. Solid curves indicate existing results from the LIGO/Virgo/KAGRA Collaboration [72,73], gravimeter monitoring of the Earth's normal modes [74], Doppler tracking of the Cassini spacecraft [75], pulsar timing by the Parkes PTA [2], and indirect constraints from $N_{\rm eff}$ [71], as well as our forecast present-day sensitivities for binary resonance searches with binary MSPs, LLR, and SLR, which are presented for the first time here. Hatching indicates the new region probed by our present-day forecasts. Dashed curves indicate our binary resonance forecast sensitivities for 2038, along with expected bounds from ET [54], LISA [5], SKA [4], and the proposed km-scale atom interferometer AION [55], as well as improved $N_{\rm eff}$ constraints [71]. Dotted curves show various potential SGWB signals in the μHz band. The purple curves indicate a possible signal associated with the common process identified by NANOGrav (NANOGrav CP) [3], while the overlaid pink curves show the inferred amplitude for the NANOGrav CP when assuming a $\Omega_{\rm gw} \sim f^{2/3}$ spectrum, as expected for supermassive binary black holes (SMBBHs). The yellow curves show two FOPT spectra at temperatures $T_* = 2$ GeV and 200 GeV, peaking at $f \approx 1\ \mu$Hz and $\approx 100\ \mu$Hz, respectively. The orange curve shows the predicted spectrum from a population of horizonless supermassive black hole (SMBH) mimickers [76]. The pale green curves show the predicted spectra from ultralight bosonic condensates around SMBHs [77], with boson masses varying from 10^{-20}eV (leftmost curve) to 10^{-15} eV (rightmost curve).

The resulting power law–integrated (PI) [52] sensitivity curves are shown in Fig. 1, alongside the sensitivities of various other current and future GW experiments [53]. For each of our binary resonance probes (MSP, LLR, and SLR), we calculate two sensitivity curves: one that reflects the data available in 2021, and one that should be achievable by 2038, by which time LISA is expected to have completed its nominal 4-year mission. By this point in the late 2030s we also anticipate sensitive SGWB searches by the Einstein

Telescope [54] (ET; a planned third-generation GW interferometer), the Square Kilometre Array [4] (SKA; a radio telescope array whose planned uses include a next-generation PTA to search for nHz GWs) and by some km-scale versions of the atom interferometers of the Atom Interferometer Observatory and Network (AION) [55] or Matter-wave Atomic Gradiometer Interferometric Sensor (MAGIS) [56] projects, which occupy the frequency band between LISA and ground-based interferometers. (There are various other constraints at lower frequencies not shown here, including those from cosmic microwave background temperature and polarization anisotropies [57,58] and spectral distortions [59], as well as potential future constraints in the frequency band we are interested in, e.g., from astrometry [60–64], helioseismology [65], modulation of GW signals [66], the μAres proposal [6], the Moon's normal modes [67,68], and high-cadence PTA observations [69,70]. However, all these constraints are either very futuristic, not applicable to stochastic GW signals, or not strong enough to be competitive with our forecasts.) The horizontal black lines in Fig. 1 show indirect constraints due to SGWB contributions to the effective number of relativistic degrees of freedom ($N_{\rm eff}$) in the early Universe [71], as probed by the cosmic microwave background (CMB) and big-bang nucleosynthesis (BBN). These lines should be interpreted differently from the other constraints that we show, as they represent bounds on the *total* subhorizon SGWB energy density (the values plotted correspond to the upper bounds on $\int d(\ln f)\Omega_{\rm gw}$ at frequencies $f \gtrsim 10^{-15}$ Hz), and only include GWs emitted before the epoch of BBN.

We find that laser-ranging experiments are already able to place cosmologically relevant bounds with present data; LLR has an expected sensitivity of $\Omega_{\rm gw} \geq 6.2 \times 10^{-6}$ at $f = 0.85\ \mu$Hz (95% confidence upper limit), while the forecast for SLR with the LAGEOS satellite is $\Omega_{\rm gw} \geq 2.4 \times 10^{-6}$ at $f = 0.15$ mHz. These forecasts, if realized, would be by far the most sensitive direct SGWB searches to date in the broad frequency band between ground-based interferometers at $f \gtrsim 10$ Hz and PTAs at $f \sim$ nHz, a full 3 orders of magnitude stronger than existing constraints from the Cassini spacecraft [75] and the Earth's normal modes [74], and competitive with indirect $N_{\rm eff}$ constraints [71], which currently set $\int d(\ln f)\Omega_{\rm gw} \leq 2.6 \times 10^{-6}$. With some reasonable assumptions about future improvements in the noise levels and data cadence of laser-ranging experiments (see the Supplemental Material [25]), these forecasts improve to $\Omega_{\rm gw} \geq 4.8 \times 10^{-9}$ for LLR and $\Omega_{\rm gw} \geq 8.3 \times 10^{-9}$ for SLR by 2038, significantly better than the $N_{\rm eff}$ constraint, which is expected to reach $\int d(\ln f)\Omega_{\rm gw} \leq 1.7 \times 10^{-7}$ by that time [71].

The frequencies $f = 0.85\ \mu$Hz and $f = 0.15$ mHz mentioned above correspond to the $n = 2$ harmonics of the Earth-Moon and Earth-LAGEOS systems, respectively. The corresponding forecast sensitivity curves are strongly

peaked in both cases, since the coupling to the $n = 2$ harmonic is by far the strongest for low-eccentricity orbits like that of the Moon ($e \approx 0.055$) and LAGEOS ($e \approx 0.0045$) [12]. The next most sensitive frequency in both cases is the $n = 1$ harmonic, which is sensitive to $\Omega_{gw} \geq 3.2 \times 10^{-4}$ for LLR and $\Omega_{gw} \geq 2.2 \times 10^{-2}$ for SLR at present, improving to $\Omega_{gw} \geq 2.5 \times 10^{-7}$ and $\Omega_{gw} \geq 7.5 \times 10^{-5}$, respectively, by 2038. (See Fig. 1 in the Supplemental Material [25] for the individual sensitivities of each harmonic of the Earth-Moon system.)

While binary pulsars are not able to compete with the laser-ranging experiments in terms of sheer sensitivity, their forecasts cover a much wider frequency band, spanning nearly five decades in frequency from ≈ 6 nHz up to ≈ 0.2 mHz. This is partly due to the range of orbital periods of various systems, and partly to the large eccentricities of many of these binaries, which gives them sensitivity to much higher harmonics. The overall binary pulsar sensitivity curves shown in Fig. 1 are computed by combining the overlapping PI curves of 215 binaries from the Australia Telescope National Facility pulsar catalog [21]. The most stringent forecast sensitivity from this combined curve is $\Omega_{gw} \geq 8.2 \times 10^{-4}$ at $f = 14$–25 nHz with present data, expected to reach $\Omega_{gw} \geq 7.5 \times 10^{-7}$ by 2038.

Figure 1 also shows various potential SGWB signals around the μHz band probed by our proposed binary resonance searches. The most important to mention here are the phase transition spectra, partly because FOPTs are a robust prediction of many well-motivated extensions to the standard model of particle physics [16–18], and partly because the spectral shape of a FOPT signal highlights the constraining power of binary resonance searches [78]. While binary resonance probes are not competitive with GW interferometers and PTAs in searching for SGWB spectra, which are roughly flat over many decades in frequency (e.g., GWs from inflation or cosmic strings), they can prove extremely useful for spectra that are confined to a narrow frequency band. FOPTs are a leading example of such a signal, producing a narrow spectrum with a peak frequency [16],

$$f_* \approx 19 \ \mu\text{Hz} \times \frac{T_*}{100 \text{ GeV}} \frac{\beta/H_*}{v_w} \left(\frac{g_*}{106.75}\right)^{1/6}, \quad (5)$$

and a peak intensity of

$$\Omega_{gw}(f_*) \approx 5.7 \times 10^{-6} \times \frac{v_w}{\beta/H_*} \left(\frac{\kappa\alpha}{1+\alpha}\right)^2 \left(\frac{g_*}{106.75}\right)^{-1/3}$$
$$\times [1 - (1 + 2\tau_{sw}H_*)^{-1/2}]. \quad (6)$$

Here, T_* is the temperature at which the FOPT occurs, α is the energy density released by the FOPT in units of the radiation density at the transition epoch, β is the inverse duration of the transition, H_* is the Hubble rate at the epoch of the transition, v_w is the bubble wall velocity, κ is an
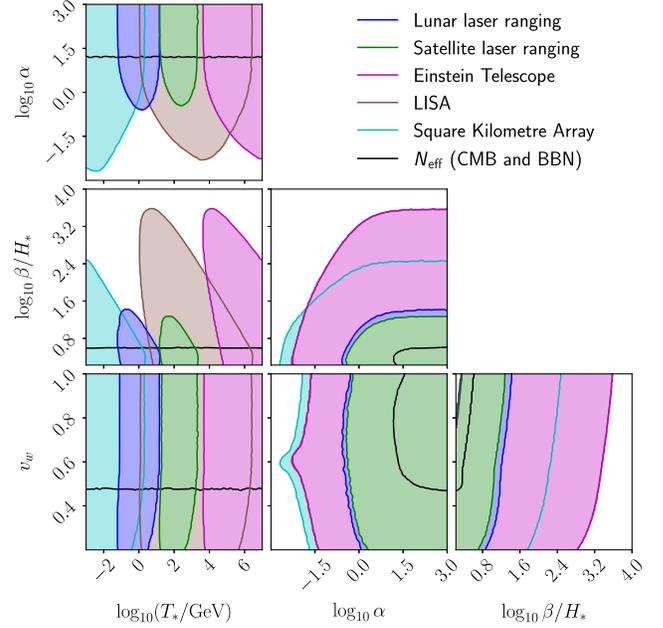
FIG. 2. Forecast exclusion regions of the FOPT parameter space for various SGWB searches at 2038 sensitivity. Here, T_* is the temperature at which the FOPT occurs, α is the energy density released by the FOPT in units of the radiation density at the transition epoch, β/H_* is the inverse duration of the transition in units of the Hubble rate at the transition epoch, and v_w is the bubble wall velocity.

efficiency parameter determined by α and v_w, and g_* is the number of relativistic degrees of freedom in the plasma, which we normalize to the standard model value, $g_*^{(\text{SM})} = 106.75$. The second line of Eq. (6) is a suppression factor due to the finite lifetime of the sound waves, τ_{sw}, which is a function of α, β, and v_w [17].

In Fig. 2, we perform a scan over the FOPT parameters $(T_*, \alpha, \beta/H_*, v_w)$ for transitions occurring between $T_* = 10^{-3}$ GeV and 10^7 GeV, identifying regions of parameter space where the corresponding SGWB signal is expected to be detected by binary resonance searches and other GW probes by 2038. We find that LLR and SLR are able to probe significant regions of the FOPT parameter space at $T_* \sim$ GeV and ~ 100 GeV, respectively. While SLR is less sensitive than LISA and will provide only complementary information, LLR will probe a region of the parameter space that is not accessible by any other planned GW experiment, thus providing a unique and valuable contribution to the search for phase transitions in the early Universe. FOPTs are only one example of a strongly peaked SGWB spectrum, but they demonstrate that binary resonance searches (and LLR in particular) have unique GW discovery potential.

Another potential SGWB signal shown in Fig. 1 is the stochastic common process identified by the NANOGrav Collaboration in their 12.5-year PTA dataset [3]. While there is not yet sufficient evidence for quadrupolar cross-pulsar

correlations to confidently interpret this signal as being due to GWs, the values inferred for its amplitude and spectral tilt are consistent with those expected for the SGWB from a population of inspiraling supermassive binary black holes [79] (SMBBHs), as well as with several more exotic interpretations [80–88]. Assuming that the spectrum seen by NANOGrav can be extrapolated into the μHz band, we find that present-day LLR data are able to probe some of the steeper spectra allowed by the NANOGrav data (roughly $\Omega_{\rm gw} \sim f^{1.8}$), which could correspond to a strongly blue-tilted [89] inflationary tensor spectrum [86,88]. If instead we assume that the NANOGrav signal follows the $\Omega_{\rm gw} \sim f^{2/3}$ scaling expected from inspiraling SMBBHs, we find that the spectrum should be detectable with 2038 LLR data. This provides further motivation for the binary resonance searches we propose, showing that LLR can probe the nature of GW signals detected in the nHz band by NANOGrav and other PTAs.

Summary and outlook.—In this Letter, we have demonstrated the potential for binary resonance searches to bridge the μHz gap in the SGWB spectrum, showing that high-precision data from pulsar timing and laser-ranging experiments may lead to the first discovery of (or stringent constraints on) the SGWB in this region. In particular, the sensitive frequency band of LLR sits almost exactly halfway between those of LISA and PTAs, and is thus highly complementary to these experiments.

As an illustrative example of the constraining power of binary resonance searches, we have considered potential SGWB spectra from FOPTs, showing that near-future LLR and SLR data will be sensitive to a broad range of FOPT models, and that LLR in particular can probe regions of the FOPT parameter space that are inaccessible to all other GW experiments. We have also shown that current and future LLR data can provide complementary information about nHz GW signals probed by PTAs, such as the candidate SGWB signal recently announced by the NANOGrav Collaboration.

Our results provide strong motivation for further work in this direction. On the theory side, there is plenty of scope to extend our formalism, either to other gravitationally bound systems (e.g., hierarchical triples, globular clusters) or other GW signal morphologies (e.g., transient and/or narrowband signals, even if not exactly on resonance). Ultimately, the most pressing future work is to develop SGWB search pipelines based on our code GWRESONANCE, allowing us to efficiently study the μHz–mHz band, perhaps even to discover GW signals waiting for us in this as-yet-unexplored regime. The history of both electromagnetic and GW astronomy gives us plenty of reasons to be optimistic about the outcomes of these searches and their potential for scientific discovery.

Our results can be reproduced using the PYTHON code GWRESONANCE, available in Ref. [24].

[*] Corresponding author.
alex.jenkins@ucl.ac.uk
Present address: Department of Physics and Astronomy, University College London, London WC1E 6BT, United Kingdom.

[1] B. P. Abbott *et al.* (LIGO Scientific, Virgo Collaborations), Observation of Gravitational Waves from a Binary Black Hole Merger, Phys. Rev. Lett. **116**, 061102 (2016).

[2] P. D. Lasky *et al.*, Gravitational-Wave Cosmology Across 29 Decades in Frequency, Phys. Rev. X **6**, 011035 (2016).

[3] Z. Arzoumanian *et al.* (NANOGrav Collaboration), The NANOGrav 12.5 yr data set: Search for an isotropic stochastic gravitational-wave background, Astrophys. J. Lett. **905**, L34 (2020).

[4] G. Janssen, G. Hobbs, M. McLaughlin, C. Bassa, A. T. Deller, M. Kramer, K. Lee, C. Mingarelli, P. Rosado, S. Sanidas, A. Sesana, L. Shao, I. Stairs, B. W. Stapper, and J. Verbiest, Gravitational wave astronomy with the SKA, Proc. Sci., AASKA14 05 (**2015**) 037 [arXiv:1501.00127].

[5] P. Amaro-Seoane *et al.* (LISA Consortium Collaboration), Laser interferometer space antenna, arXiv:1702.00786.

[6] A. Sesana *et al.*, Unveiling the gravitational universe at μHz frequencies, Exp. Astron. **51**, 1333 (2021).

[7] B. Bertotti, Is the solar system gravitationally closed?, Astrophys. Lett. **14**, 51 (1973), https://ui.adsabs.harvard.edu/abs/1973ApL....14...51B/abstract.

[8] V. N. Rudenko, Test bodies under the effect of gravitational radiation, Sov. Astron. **19**, 270 (1975), https://ui.adsabs.harvard.edu/abs/1975SvA....19..270R/abstract.

[9] M. S. Turner, Influence of a weak gravitational wave on a bound system of two point-masses, Astrophys. J. **233**, 685 (1979).

[10] B. Mashhoon, B. J. Carr, and B. L. Hu, The influence of cosmological gravitational waves on a Newtonian binary system, Astrophys. J. **246,** 569 (1981).

[11] L. Hui, S. T. McWilliams, and I.-Sheng Yang, Binary systems as resonance detectors for gravitational waves, Phys. Rev. D **87,** 084009 (2013).

[12] D. Blas and A. C. Jenkins, companion paper, Detecting stochastic gravitational waves with binary resonance, Phys. Rev. D **105,** 064021 (2022).

[13] N. Aghanim *et al.* (Planck Collaboration), Planck 2018 results. VI. Cosmological parameters, Astron. Astrophys. **641,** A6 (2020).

[14] C. D. Murray and S. F. Dermott, *Solar System Dynamics* (Cambridge University Press, Cambridge, England, 2000).

[15] T. Regimbau, The astrophysical gravitational wave stochastic background, Res. Astron. Astrophys. **11,** 369 (2011).

[16] C. Caprini, M. Hindmarsh, S. Huber, T. Konstandin, J. Kozaczuk, G. Nardini, J. M. No, A. Petiteau, P. Schwaller, G. Servant, and D. J. Weir, Science with the space-based interferometer eLISA. II: Gravitational waves from cosmological phase transitions, J. Cosmol. Astropart. Phys. 04 (2016) 001.

[17] C. Caprini, M. Chala, G. C. Dorsch, M. Hindmarsh, S. J. Huber, T. Konstandin, J. Kozaczuk, G. Nardini, J. M. No, K. Rummukainen, P. Schwaller, G. Servant, A. Tranberg, and D. J. Weir, Detecting gravitational waves from cosmological phase transitions with LISA: An update, J. Cosmol. Astropart. Phys. 03 (2020) 024.

[18] C. Caprini and D. G. Figueroa, Cosmological backgrounds of gravitational waves, Classical Quantum Gravity **35,** 163001 (2018).

[19] The Fokker-Planck equation is clearly linear in W. In this context, "nonlinear" means that the drift vector and diffusion matrix are functions of the orbital elements, giving rise to interesting effects such as noise-induced drift [20].

[20] H. Risken, *The Fokker-Planck Equation: Methods of Solution and Applications*, 2nd ed. (Springer-Verlag, Berlin, 1989).

[21] R. N. Manchester, G. B. Hobbs, A. Teoh, and M. Hobbs, The Australia Telescope National Facility pulsar catalogue, Astron. J. **129,** 1993 (2005).

[22] T. W. Murphy, Lunar laser ranging: the millimeter challenge, Rep. Prog. Phys. **76,** 076901 (2013).

[23] I. Ciufolini, A. Paolozzi, E. C. Pavlis, R. Koenig, J. Ries, V. Gurzadyan, R. Matzner, R. Penrose, G. Sindoni, C. Paris, H. Khachatryan, and S. Mirzoyan, A test of general relativity using the LARES and LAGEOS satellites and a GRACE Earth gravity model, Eur. Phys. J. C **76,** 120 (2016).

[24] https://github.com/alex-c-jenkins/gw-resonance.

[25] See Supplemental Material at http://link.aps.org/supplemental/10.1103/PhysRevLett.128.101103, which includes Refs. [25–50], for further details about our procedure for integrating the Fokker-Planck equation and computing sensitivity forecasts, as well as details on the FOPT spectra we use to generate Fig. 2, so that all of our results may be reproduced using our publicly available code GWRESONANCE. We also discuss how to obtain long-timescale

SGWB constraints using the present-day orbital parameters of Solar System bodies.

[26] E. Poisson and C. M. Will, *Gravity: Newtonian, Post-Newtonian, Relativistic* (Cambridge University Press, Cambridge, England, 2014).

[27] P. C. Peters and J. Mathews, Gravitational radiation from point masses in a Keplerian orbit, Phys. Rev. **131,** 435 (1963).

[28] R. Blandford and S. A. Teukolsky, Arrival-time analysis for a pulsar in a binary system, Astrophys. J. **205,** 580 (1976).

[29] G. Casella and R. L. Berger, *Statistical Inference*, 2nd ed. (Duxbury, 2002).

[30] A. Lyne, B. Stappers, M. Keith, P. Ray, M. Kerr, F. Camilo, and T. Johnson, The binary nature of PSR J2032 + 4127, Mon. Not. R. Astron. Soc. **451,** 581 (2015).

[31] A. A. Abdo, M. Ackermann, M. Ajello *et al.* (Fermi-LAT Collaboration), Detection of 16 gamma-ray pulsars through blind frequency searches using the fermi LAT, Science **325,** 840 (2009).

[32] M. Kramer, I. H. Stairs, R. N. Manchester, M. A. McLaughlin, A. G. Lyne, R. D. Ferdman, M. Burgay, D. R. Loreimer, A. Possenti, N. D'Amico, J. M. Sarkissian, G. B. Hobbs, J. E. Reynolds, P. C. C. Freire, and F. Camilo, Tests of general relativity from timing the double pulsar, Science **314,** 97 (2006).

[33] J. M. Weisberg and Y. Huang, Relativistic measurements from timing the binary pulsar PSR B1913 + 16, Astrophys. J. **829,** 55 (2016).

[34] B. A. Jacoby, P. B. Cameron, F. A. Jenet, S. B. Anderson, R. N. Murty, and S. R. Kulkarni, Measurement of orbital decay in the double neutron star binary PSR B2127 + 11C, Astrophys. J. Lett. **644,** L113 (2006).

[35] E. Fonseca, I. H. Stairs, and S. E. Thorsett, A comprehensive study of relativistic gravity using PSR B1534 + 12, Astrophys. J. **787,** 82 (2014).

[36] H. T. Haniewicz, R. D. Ferdman, P. C. C. Freire, D. J. Champion, K. A. Bunting, D. R. Lorimer, and M. A. McLaughlin, Precise mass measurements for the double neutron star system J1829 + 2456, Mon. Not. R. Astron. Soc. **500,** 4620 (2020).

[37] M. H. van Kerkwijk and S. R. Kulkarni, A massive white dwarf companion to the eccentric binary pulsar system PSR B2303 + 46, Astrophys. J. Lett. **516,** L25 (1999).

[38] V. M. Kaspi, M. Bailes, R. N. Manchester, B. W. Stappers, and J. F. Bell, Evidence from a precessing pulsar orbit for a neutron-star birth kick, Nature (London) **381,** 584 (1996).

[39] P. C. C. Freire, C. G. Bassa, N. Wex, I. H. Stairs, D. J. Chamion, S. M. Ransom, P. Lazarus, V. M. Kaspi, J. W. T. Hessels, M. Kramer, J. M. Cordes, J. P. W. Verbiest, P. Podsiadlowski, D. J. Nice, J. S. Deneva, D. R. Lorimer, B. W. Stappers, M. A. McLaughlin, and F. Camilo, On the nature and evolution of the unique binary pulsar J1903 + 0327, Mon. Not. R. Astron. Soc. **412,** 2763 (2011).

[40] E. C. Madsen, I. H. Stairs, M. Kramer, F. Camilo, G. B. Hobbs, G. H. Janssen, A. G. Lyne, R. N. Manchester, A. Possenti, and B. W. Stappers, Timing the main-sequence-star binary pulsar J1740-3052, Mon. Not. R. Astron. Soc. **425,** 2378 (2012).

[41] J. C. A. Miller-Jones, A. T. Deller, R. M. Shannon, R. Dodson, J. Moldón, M. Ribó, G. Dubus, S. Johnston, J. M. Paredes, S. M. Ransom, and J. A. Tomsick, The geometric distance and binary orbit of PSR B1259–63, Mon. Not. R. Astron. Soc. **479,** 4849 (2018).

[42] K. Liu, J. P. W. Verbiest, M. Kramer, B. W. Stappers, W. van Straten, and J. M. Cordes, Prospects for high-precision pulsar timing, Mon. Not. R. Astron. Soc. **417,** 2916 (2011).

[43] ILRS, International laser ranging service: Lageos, https://ilrs.gsfc.nasa.gov/missions/satellite_missions/current_missions/lag1_general.html (accessed May 2021).

[44] M. A. Fedderke, P. W. Graham, and S. Rajendran, Gravity gradient noise from asteroids, Phys. Rev. D **103,** 103017 (2021).

[45] JPL, Small-body database browser, https://ssd.jpl.nasa.gov/sbdb.cgi (accessed May 2021).

[46] K. Schmitz, New sensitivity curves for gravitational-wave signals from cosmological phase transitions, J. High Energy Phys. 01 (2021) 097.

[47] J. R. Espinosa, T. Konstandin, J. M. No, and G. Servant, Energy budget of cosmological first-order phase transitions, J. Cosmol. Astropart. Phys. 06 (2010) 028.

[48] J. Ellis, M. Lewicki, and J. M. No, Gravitational waves from first-order cosmological phase transitions: Lifetime of the sound wave source, J. Cosmol. Astropart. Phys. 07 (2020) 050.

[49] V. Desjacques, E. Grishin, and Y. B. Ginat, Axion oscillations in binary systems: angle-action surgery, Astrophys. J. **901,** 85 (2020).

[50] J. M. Armaleo, D. López Nacir, and F. R. Urban, Pulsar timing array constraints on spin-2 ULDM, J. Cosmol. Astropart. Phys. 09 (2020) 031.

[51] D. Blas, D. L. Nacir, and S. Sibiryakov, Secular effects of ultralight dark matter on binary pulsars, Phys. Rev. D **101,** 063016 (2020).

[52] E. Thrane and J. D. Romano, Sensitivity curves for searches for gravitational-wave backgrounds, Phys. Rev. D **88,** 124032 (2013).

[53] Note that these curves represent the sensitivity to a power-law SGWB, $\Omega_{gw}(f) \sim f^\alpha$ with $|\alpha| \leq 10$, and that sufficiently sharply peaked spectra might overlap these curves without being detected; see the Supplemental Material [25] for further details.

[54] M. Punturo et al., The Einstein Telescope: A third-generation gravitational wave observatory, Classical Quantum Gravity **27,** 194002 (2010).

[55] L. Badurina et al., AION: An atom interferometer observatory and network, J. Cosmol. Astropart. Phys. 05 (2020) 011.

[56] M. Abe et al., Matter-wave atomic gradiometer interferometric sensor (MAGIS-100), Quantum Sci. Technol. **6,** 044003 (2021).

[57] P. A. R. Ade et al. (BICEP2, Planck Collaborations), Joint Analysis of BICEP2/Keck Array and Planck Data, Phys. Rev. Lett. **114,** 101301 (2015).

[58] T. Namikawa, S. Saga, D. Yamauchi, and A. Taruya, CMB constraints on the stochastic gravitational-wave background at Mpc scales, Phys. Rev. D **100,** 021303(R) (2019).

[59] T. Kite, A. Ravenni, S. P. Patil, and J. Chluba, Bridging the gap: Spectral distortions meet gravitational waves, Mon. Not. R. Astron. Soc. **505,** 4396 (2021).

[60] C. J. Moore, D. P. Mihaylov, A. Lasenby, and G. Gilmore, Astrometric Search Method for Individually Resolvable Gravitational Wave Sources with Gaia, Phys. Rev. Lett. **119,** 261102 (2017).

[61] J. Darling, A. E. Truebenbach, and J. Paine, Astrometric limits on the stochastic gravitational wave background, Astrophys. J. **861,** 113 (2018).

[62] Y. Wang, K. Pardo, T.-C. Chang, and O. Doré, Gravitational wave detection with photometric surveys, Phys. Rev. D **103,** 084007 (2021).

[63] J. Garcia-Bellido, H. Murayama, and G. White, Exploring the early Universe with Gaia and Theia, J. Cosmol. Astropart. Phys. 12 (2021) 023.

[64] S. Aoyama, D. Yamauchi, M. Shiraishi, and M. Ouchi, Gaia 400,894 QSO constraint on the energy density of low-frequency gravitational waves, arXiv:2105.04039.

[65] I. Lopes and J. Silk, Nearby stars as gravitational wave detectors, Astrophys. J. **807,** 135 (2015).

[66] M. J. Bustamante-Rosell, J. Meyers, N. Pearson, C. Trendafilova, and A. Zimmerman, Gravitational wave timing array, Phys. Rev. D **105,** 044005 (2022).

[67] J. Harms et al. (LGWA Collaboration), Lunar gravitational-wave antenna, Astrophys. J. **910,** 1 (2021).

[68] K. Jani and A. Loeb, Gravitational-wave lunar observatory for cosmology, J. Cosmol. Astropart. Phys. 06 (2021) 044.

[69] B. B. P. Perera et al., Improving timing sensitivity in the microhertz frequency regime: Limits from PSR J1713 + 0747 on gravitational waves produced by super-massive black-hole binaries, Mon. Not. R. Astron. Soc. **478,** 218 (2018).

[70] Y. Wang, S. D. Mohanty, and Z. Cao, Extending the frequency reach of pulsar timing array based gravitational wave search without high cadence observations, Astrophys. J. Lett. **907,** L43 (2021).

[71] L. Pagano, L. Salvati, and A. Melchiorri, New constraints on primordial gravitational waves from Planck 2015, Phys. Lett. B **760,** 823 (2016).

[72] R. Abbott et al. (LIGO Scientific, Virgo, KAGRA Collaborations), Upper limits on the isotropic gravitational-wave background from Advanced LIGO and Advanced Virgo's third observing run, Phys. Rev. D **104,** 022004 (2021).

[73] R. Abbott et al. (LIGO Scientific, Virgo, KAGRA Collaborations), Data for "Upper limits on the isotropic gravitational-wave background from Advanced LIGO's and Advanced Virgo's third observing run", https://dcc.ligo.org/LIGO-G2001287/public (2021).

[74] M. Coughlin and J. Harms, Constraining the gravitational wave energy density of the Universe using Earth's ring, Phys. Rev. D **90,** 042005 (2014).

[75] J. W. Armstrong, L. Iess, P. Tortora, and B. Bertotti, Stochastic gravitational wave background: Upper limits in the 10^{-6} Hz–10^{-3} Hz band, Astrophys. J. **599,** 806 (2003).

[76] E. Barausse, R. Brito, V. Cardoso, I. Dvorkin, and P. Pani, The stochastic gravitational-wave background in the absence of horizons, Classical Quantum Gravity **35,** 20LT01 (2018).

[77] R. Brito, S. Ghosh, E. Barausse, E. Berti, V. Cardoso, I. Dvorkin, A. Klein, and P. Pani, Stochastic and Resolvable Gravitational Waves from Ultralight Bosons, Phys. Rev. Lett. **119,** 131101 (2017).

[78] Here, we focus on the SGWB signal due to sound waves in the plasma, as this is expected to be the dominant contribution for most FOPTs [17].

[79] H. Middleton, A. Sesana, S. Chen, A. Vecchio, W. Del Pozzo, and P. A. Rosado, Massive black hole binary systems and the NANOGrav 12.5 yr results, Mon. Not. R. Astron. Soc. **502**, L99 (2021).

[80] J. Ellis and M. Lewicki, Cosmic String Interpretation of NANOGrav Pulsar Timing Data, Phys. Rev. Lett. **126**, 041304 (2021).

[81] S. Blasi, V. Brdar, and K. Schmitz, Has NANOGrav Found First Evidence for Cosmic Strings?, Phys. Rev. Lett. **126**, 041305 (2021).

[82] V. Vaskonen and H. Veermäe, Did NANOGrav See a Signal from Primordial Black Hole Formation?, Phys. Rev. Lett. **126**, 051303 (2021).

[83] V. De Luca, G. Franciolini, and A. Riotto, NANOGrav Data Hints at Primordial Black Holes as Dark Matter, Phys. Rev. Lett. **126**, 041303 (2021).

[84] W. Buchmuller, V. Domcke, and K. Schmitz, From NANO-Grav to LIGO with metastable cosmic strings, Phys. Lett. B **811**, 135914 (2020).

[85] W. Ratzinger and P. Schwaller, Whispers from the dark side: Confronting light new physics with NANOGrav data, SciPost Phys. **10**, 047 (2021).

[86] S. Vagnozzi, Implications of the NANOGrav results for inflation, Mon. Not. R. Astron. Soc. **502**, L11 (2021).

[87] A. Neronov, A. Roper Pol, C. Caprini, and D. Semikoz, NANOGrav signal from magnetohydrodynamic turbulence at the QCD phase transition in the early Universe, Phys. Rev. D **103**, L041302 (2021).

[88] S. Kuroyanagi, T. Takahashi, and S. Yokoyama, Blue-tilted inflationary tensor spectrum and reheating in the light of NANOGrav results, J. Cosmol. Astropart. Phys. 01 (2021) 071.

[89] Such spectra can avoid the existing LVK and N_{eff} constraints if one allows for a nonstandard thermal history [88].

[90] C. R. Harris et al., Array programming with NumPy, Nature (London) **585**, 357 (2020).

[91] P. Virtanen et al. (SciPy1.0 Contributors), SciPy1.0: Fundamental algorithms for scientific computing in Python, Nat. Methods **17**, 261 (2020).

[92] D. Foreman-Mackey, D. W. Hogg, D. Lang, and J. Goodman, emcee: The MCMC Hammer, Publ. Astron. Soc. Pac. **125**, 306 (2013).

[93] J. D. Hunter, Matplotlib: A 2d graphics environment, Comput. Sci. Eng. **9**, 90 (2007).

[94] D. Foreman-Mackey, corner.py: Scatterplot matrices in python, J. Open Source Softwaare **1**, 24 (2016).